

1 **Towards monitoring large and complex wildlife aggregations with drones**

2

3 Mitchell Lyons\*, Kate Brandis, Nick Murray, John Wilshire, Justin McCann, Richard

4 Kingsford & Corey Callaghan

5

6 Centre for Ecosystem Science, School of Biological, Earth and Environmental Sciences,

7 UNSW Australia, Sydney Australia 2052

8 \* corresponding author: mitchell.lyons@unsw.edu.au

9

10 **Running title:** Monitoring wildlife aggregations with drones

11

12 **Key words** (depending on title): remote sensing, modelling, monitoring, aerial vehicle,

13 breeding, colonial, waterbird, automated detection, machine learning

14

15

16 **NOTE: This is a preprint, still under consideration for publication, and this version has**

17 **not yet undergone peer review**

18 **Abstract**

- 19 • Recent advances in drone technology have rapidly led to their increased use for  
20 monitoring and managing wildlife populations. Despite demonstration of their relative  
21 advantages over traditional ecological methods, we have not seen a shift to their use  
22 more generally by ecologists and managers, particularly at large spatial scale and for  
23 environments with high biotic or abiotic complexity
- 24 • In this paper we present a generalisable semi-automated approach that first uses a  
25 machine learning approach to map targets of interest in drone imagery, and then a  
26 predictive modelling approach that estimates target counts. We use a case study of  
27 four large breeding waterbird colonies, ranging in size from ~20,000 to ~250,000  
28 birds, where the ecological goal was to map and count bird nests. Google Earth  
29 Engine was used for the nest mapping, so users do not require significant local  
30 computing resources, and R for the nest count modelling.
- 31 • The approach we developed was able to be applied to all four colonies without any  
32 modification to the mapping or modelling routine, and was able to deal with large  
33 amounts of variation in nest size, shape, colour and density, as well as variation in  
34 background type and heterogeneity (vegetation, water, sand, soil etc.). Our approach  
35 estimated nest numbers at about the same accuracy as manual counting from the  
36 drone-imagery
- 37 • Our approach represents a significant improvement in cost-benefit for monitoring  
38 large and complex aggregations of wildlife, and a new potential solution for  
39 monitoring very large and complex aggregations where ground counts are virtually  
40 impossible. Importantly our approach also has a relatively low technical threshold for  
41 user's application to their own data. All code used for mapping and modelling nests is  
42 provided and we also provide an online web-app for users to explore the drone  
43 imagery and mapping predictor layers.

## 44 **1 Introduction**

45 Recent advances in technology offer the potential to improve field methods for rapidly and  
46 effectively monitoring biodiversity (Pimm *et al.* 2015). Among these advances is the use of  
47 aerial vehicles, or drones, that can carry remote sensing instrumentation (Anderson & Gaston  
48 2013). The growing use of drones to capture image data has been driven by their relative ease  
49 of use, allowing people from a range of fields to capture extremely high spatial resolution  
50 data at a temporal resolution tailored to their needs. This has led to much excitement about  
51 the use of drones for wildlife monitoring (e.g.(Chabot & Bird 2015)), and novel applications  
52 for monitoring both populations and features of a range of different fauna, including birds  
53 (Chabot & Francis 2016; Hodgson *et al.* 2018), elephants (Vermeulen *et al.* 2013), crocodiles  
54 (Evans *et al.* 2016) and marine mammals (Seymour *et al.* 2017).

55

56 Given their ability to collect high quality data in close proximity to large aggregations of  
57 wildlife, drones offer an attractive opportunity to improve methods for monitoring population  
58 and status. The relative advantages of aerial counting for these activities to complement  
59 ground surveys is long established, including reduced detection error, increased precision,  
60 ability to retrospectively analyse data and reduced observer effects. For example, Fraser *et al.*  
61 (1999) used aerial images of penguin colonies from a kite and Boyd (2000) used aerial  
62 (aeroplane) photography of geese flocks to show that aerial counting was more accurate and  
63 precise than ground counting. Recently, the same advantages over ground counts have been  
64 demonstrated with aerial photos captured with drones (Hodgson *et al.* 2018). However,  
65 application of drones in this context has generally been limited to either following sporadic  
66 individuals or, apart from a few exceptions (Chabot & Bird 2012; Chabot, Craik & Bird  
67 2015; Afán, Máñez & Díaz-Delgado 2018), monitoring fairly small aggregations (i.e. < 5-  
68 10,000 individuals).

69

70 At large spatial scales (km's) and for large aggregations (e.g. >5,000-10,000 individuals),  
71 aerial surveys have long been seen as the only feasible methodology for providing  
72 information on parameters like counts of individuals, breeding-pairs and nests (Caughley  
73 1977; Kingsford & Porter 2009). High altitude imagery from aeroplanes allows large areas, if  
74 not whole aggregations, to be captured in single images. (Boyd 2000) demonstrated counting  
75 of multiple large flocks of geese from aerial imagery, noting that ~30 photos captured flocks  
76 of ~10,000 geese. Using drones, large aggregations require many thousands of photos to  
77 provide coverage.

78

79 Manually counting targets of interest (e.g. individual animals, breeding-pairs, nests) from  
80 aerial images, regardless of capture platform, is laborious. This has driven the development of  
81 automated or semi-automated counting approaches (Chabot & Francis 2016; Hollings *et al.*  
82 2018), aided by the widespread availability of increased computing power, growing computer  
83 literacy and new methods. Current approaches typically involve spectral thresholding  
84 (Chabot & Bird 2012; Seymour *et al.* 2017), point process algorithms (Descamps *et al.* 2011)  
85 or combinations of spectral properties and predictive modelling (Hodgson *et al.* 2018). These  
86 methods rely on high contrast (i.e. dark animals on light backgrounds or light animals on dark  
87 backgrounds) and consistency in the shape and colour of the targets (Hollings *et al.* 2018).  
88 They are generally only applicable when the spectral and structural characteristics of the  
89 animals (in the images) are unique compared to the rest of the image (Chabot & Francis  
90 2016). More recently, remote sensing-based methods have been used to overcome challenges  
91 with low contrast and high variation among target objects (Groom *et al.* 2011; Drever *et al.*  
92 2015; Liu, Chen & Wen 2015; Afán, Máñez & Díaz-Delgado 2018; Chabot, Dillon & Francis  
93 2018).

94

95 Notwithstanding the promise of these applications, several major shortcomings have been  
96 reported, including in their ability to i) scale to cases or applications with large spatial  
97 extents, ii) deal with large numbers of highly mobile individuals or iii) account for complex  
98 environmental conditions (Baxter & Hamilton 2018; Hollings *et al.* 2018). A common  
99 example of when these three limitations are encountered is for large breeding bird colonies,  
100 which we use as case studies in this paper. Despite the interest in automated methods for  
101 counting aggregations of birds, there has not been a shift towards their use by ecologists and  
102 managers for monitoring bird colonies (Chabot & Francis 2016), and manual interpretation  
103 methods remains popular (Buckland *et al.* 2012; Drever *et al.* 2015).

104

105 Hollings *et al.* (2018) highlighted that two key reasons for this are that most methods have  
106 only been demonstrated 1) at small spatial scales relative to real-world applications, even if  
107 the number of individuals is very large, and 2) in homogenous environments that do not  
108 represent the complexity likely to be found in real world applications. Additionally,  
109 automated methods are often sought for larger colonies or groups, when the methods become  
110 cost-effective (Chabot & Francis 2016), and these larger groups usually present the complex  
111 conditions and image characteristics that inhibit generalisation of automated methods. These  
112 include: structural and spectral differences of birds and nests at various breeding stages (e.g.  
113 empty nests, adult/juvenile/chick/egg occupied nest, variable nest material, variable nest  
114 shape and arrangement); birds that do not stay stationary during nesting; differences in the  
115 structural and spectral properties of the background imagery (mud, sand, water, live/dead  
116 vegetation etc.); or variable population density across space.

117

118 A disconnect between the methods literature and ecological applications has also inhibited  
119 uptake (Chabot & Francis 2016). The direct barrier in terms of technical skills to implement  
120 and modify automated methods is only part of the issue. Automated methods almost

121 exclusively focus on counting individuals, yet often, the primary biological parameter of  
122 interest is not individuals but the number or status of breeding-pairs or nests (Chabot, Craik  
123 & Bird 2015; Sarda-Palomera *et al.* 2017; Callaghan *et al.* 2018). Considerations of  
124 detectability and ecological context are a critical consideration during planning (Baxter &  
125 Hamilton 2018). Historically, individual counts have sometimes been used as a surrogate for  
126 these parameters, but with increased spatial resolution of drone-based imagery, these salient  
127 features like nest counts (Chabot, Craik & Bird 2015; Lyons *et al.* 2018a) and nesting success  
128 (Sarda-Palomera *et al.* 2017) can be directly quantified.

129

130 In this paper, we develop a framework for mapping and counting nests in large colonies of  
131 breeding birds from drone acquired imagery. We use the case study of colonial waterbird  
132 breeding colonies because they contain several of the key challenges currently inhibiting  
133 uptake of drone-based methods, including i) targets that vary in colour in shape, ii) spatially  
134 large and complex environments including dry and inundated land and vegetation, and iii)  
135 many thousands of highly mobile animals that cannot be contained to single images. We  
136 developed a compartmentalised workflow that focuses on ecological outcomes that can be  
137 adapted to different methods and software platforms. We particularly focus on a methodology  
138 that is transferrable between target types and that has a relatively low technical ability  
139 threshold. We captured imagery over four breeding waterbird colonies in New South Wales,  
140 Australia, ranging in size from ~20,000 to >200,000 birds. Our framework was developed on  
141 some of the largest ever bird colonies to be surveyed by drone, and includes flight planning,  
142 image acquisition and processing, manual and automated methods for mapping and  
143 accurately counting nests. While this paper uses bird colonies as the case study, our  
144 methodology requires only minimal technical expertise, and should generalise to monitoring  
145 challenges for other large and complex biological phenomena.

146

## 147 **2 Data & methods**

148 The primary motivation in this study was mapping and counting nests for breeding colonial  
149 waterbirds. The key requirements for our methodology was that it must work on both small  
150 (~10,000 – 20,000 birds) and large (200,000+ birds) colonies and require no changes to the  
151 mapping and modelling implementations, and that there should be a low technical threshold  
152 for modifying the approach. We developed a modular approach that involved 1) drone image  
153 surveys of four large breeding colonies, 2) manual counting of nests for training and  
154 validation, 3) a machine learning mapping method to map nests from drone imagery and 4) a  
155 predictive modelling method to estimate total nests numbers.

156

### 157 *2.1 Study location and bird colony details*

158 Straw-necked Ibis (*Threskiornis spinicollis*) are a nomadic bird species of Australia, and form  
159 very large breeding colonies when ecological conditions are favourable. We surveyed four  
160 colonies: *Merrimajeel*, *Zoo Paddock*, *Eulimbah* and *Block Bank* (location and size details in  
161 Table 1). Coordinating with on-ground ecologists, we attempted to survey the colonies at  
162 around their maximum size, to provide corresponding estimates of population. Straw-necked  
163 Ibis typically make their nests in flooded wetlands and flood plains, making use of inundated  
164 vegetation as nesting material raised above ground/water level. Their nests can be single  
165 isolated nests or in ‘clumps’ of up to 100-200 nests. The nests are generally round or oblong  
166 in shape, but are often irregular when in large clumps. The nests are typically made of  
167 trampled vegetation, so can be dark green to brown, and as they continue to be used they  
168 become white with guano, until eventually they are abandoned and lose any obvious structure  
169 or colour. Additionally, at any time point the nests may be empty, occupied by adults, eggs or  
170 juveniles, or some combination thereof. A colony usually has a mixture of nest and juvenile  
171 ages. The vast majority of birds in the colony were Straw-necked Ibis, which are a dark  
172 glossy blue-black colour on their back and wings, and have a white underside (black when

173 viewed from above). There were also small numbers (<500-1000) of Australian White Ibis  
174 (*T. Molucca*), Glossy Ibis (*Plegadis falcinellus*) and Spoonbills (*Platalea spp.*). Figure 1  
175 shows some example imagery of birds and nests at the colonies.

176

## 177 *2.2 Drone data and processing*

178 Drone image data were collected during Spring and Summer of 2016 and 2017 (exact dates in  
179 Table 1). The data was collected using a DJI Phantom 3 Professional quad-copter, with the  
180 stock single sensor red/green/blue (RGB) camera. Colonies are typically located within large  
181 flooded extents, so multi-rotor drones are the only option, due to a lack of landing area for  
182 fixed-wing drones. An amphibious vehicle or canoe was used to enter the colonies, on which  
183 a platform can be set up to launch a drone. Flights were conducted using parallel flight lines  
184 at an altitude of ~100 m above take off and at a speed of 5-10 m/s (Lyons *et al.* 2019). We  
185 aimed to acquire imagery with ~70% forward and lateral overlap to ensure adequate photo  
186 overlap for post-processing. Depending on weather and environmental conditions, we were  
187 able to survey between 10-40 hectares per flight, so multiple flights were required to survey  
188 each of the colonies. Animal ethics and interaction considerations can be found in Lyons *et*  
189 *al.* (2018a), and a more detailed protocol for drone-based monitoring of waterbird colonies in  
190 Lyons *et al.* (2019).

191

192 The drone imagery was processed using the commercial software Pix4DMapper (v4.19,  
193 Pix4D SA). Pix4D uses a photogrammetry technique called ‘structure from motion’ which  
194 uses points identifiable in overlapping images to generate a 3D point cloud reconstruction of  
195 the landscape. The 3D information is then used to generate a digital surface model and an  
196 orthorectified image mosaic. Only standard accuracy GPS (5 – 10 m accuracy) was used for  
197 georeferencing. This results in some error in absolute geographic location, but this did not



198 concern us since we were only interested in identifying the relative position of features in the  
199 image mosaics.

200

### 201 *2.3 Semi-automated approach*

202 The objective for the bird colonies in our study was mapping and counting of nests. This was  
203 to support the broader ecological goal of delineating the spatial organisation of nests and  
204 nesting success in response to environmental drivers. While estimates of the population of  
205 individuals is of general interest, this number is more variable over short time periods  
206 compared to nest numbers. Additionally, ibis are quite mobile during nesting (e.g. at the  
207 Merrimajeel colony, there was usually >10,000 birds in the air), so counting individuals from  
208 drone-based imagery was not expected to produce accurate results (i.e. double-counting).

209

210 As described above, the nests are highly variable in shape and colour, and sometimes have  
211 low contrast to the surrounding environment (Fig. 1). We initially tested a point process  
212 algorithm ((Descamps *et al.* 2011); could not handle large data sizes), an object-based image  
213 analysis routine (*sensu* Chabot, Dillon and Francis (2018); difficult to identify >3,000-5,000  
214 nests with one ruleset) and a machine learning/modelling approach ((Hodgson *et al.* 2018);  
215 could not identify >1,000 nests with one parameterisation – see Data accessibility for access  
216 to modified Matlab routine). Being unable to find generalised combinations of parameters  
217 that worked either within or between the colonies we surveyed was in line with recent  
218 findings on the limitations of automated and semi-automated methods (Hollings *et al.* 2018).  
219 We thus aimed to develop a modular approach that could adapt to variable target properties  
220 as well as be scaled to large spatial extents across multiple colonies. This involved first  
221 mapping the area of nests using a remote sensing approach, and then estimating the number  
222 of nests using a predictive modelling approach.

223

224 *2.3.1 Manual training and validation set*

225 A comprehensive training and validation data set is critical for developing counting methods,  
226 we thus decided to manually count all the nests in the imagery over the colonies. We  
227 developed a systematic approach to compiling the manual nest counts, which involved  
228 splitting each colony into a grid of 50 x 50 m quadrats, and digitally annotating every visible  
229 nest. We used this gridded method for two reasons: 1) it enabled an observer to sequentially  
230 work through the whole colony, while reducing distraction (and computer memory overhead)  
231 from surrounding areas, and 2) it allowed us to simulate real-world scenarios when users  
232 would choose only a limited number of training quadrats to manually count nests. During the  
233 field work, we counted nests (in situ) for GPS-tagged clumps at each colony, and we used  
234 these data to test the accuracy of the drone-based manual counting.

235

236 *2.3.2 Nest mapping*

237 We applied a supervised machine learning approach to map nest area at each colony. We  
238 defined nest area as any material or bird that constituted a nest or nest clump. Motivated by  
239 its robustness to redundant predictor variables, we used a random forest classifier (Breiman  
240 2001). Random forests are a machine learning algorithm that uses information from a training  
241 set and a suite of relevant predictor variables to predict class membership of all the image  
242 pixels in the study area. Random forests are particularly robust to redundant predictors, which  
243 is an important feature given that all data came from the one sensor. This allowed us to  
244 include many different image-based predictor variables without having to alter the approach  
245 for each colony.

246

247 Since all nests had been manually identified, we implemented a sampling method to choose a  
248 subset of nests to train the random forest classifier. We randomly placed points across the  
249 colony that were at least 30 m apart, and then randomly chose a number of those points to

250 train the classifier. To approximate the 50 x 50 m quadrats, a 30 m buffer was placed around  
251 each of the chosen points, and all manually counted nests within the buffer were selected as  
252 training nests. The classifier also requires non-target features, so ‘non-nest’ points were  
253 randomly spread across the remaining colony; 1000 points for the smaller colonies (Eulimbah  
254 and Block Bank) and 10,000 points for the larger colonies (Merrimajeel and Zoo Padock).

255

256 We derived a number of arithmetic and textural metrics from the red, green and blue channels  
257 ( $r, g, b$  respectively) in the drone data to use as predictor variables in the random forest  
258 classification. These included: a ‘white’ index  $\frac{b+g}{r}$ ; a Laplacian-8 edge-detection kernel on  
259 the ‘white’ metric; an RGB vegetation index  $\frac{g-r}{g+r}$  (Bendig *et al.* 2015); a ‘green brightness’  
260 index  $\frac{g}{b+g+r}$ ; the ‘contrast’, ‘variance’, ‘inverse difference moment’ and ‘shade’ texture  
261 metrics from the Gray Level Co-occurrence Matrix (Haralick 1979) applied to each of the  
262 ‘white’ index and blue band; the standard deviation within a 2 m and 7 m radius of each pixel  
263 applied to the ‘shade’ metric and vegetation index; and a 1<sup>st</sup> and 2<sup>nd</sup> order difference of  
264 gaussians (Polakowski *et al.* 1997) on the ‘shade’ metric.

265

266 The training data set was compiled by extracting the pixel values for each image metric layer  
267 within a 10 cm buffer around each training nest and non-nest point, so the random forest  
268 classifier was a binary nest and non-nest classification. The algorithm was parameterised with  
269 500 trees and a minimum leaf population of 10. We implemented the classification in the  
270 Google Earth Engine (Gorelick *et al.* 2017), as it allowed a seamless prototyping,  
271 visualisation and production environment for processing the large high resolution image data  
272 sets. Any contiguous areas less than 0.03 m<sup>2</sup> were removed (classification noise considered  
273 unlikely to be bird nests) and exported from the Earth Engine. The Google Earth Engine is  
274 freely available to anyone, and we provide the code required to run the classifications, along

275 with an interactive web-app to explore some drone data, predictor layers and nest  
276 classification interactively (see Data accessibility section).

277

### 278 *2.3.2 Nest counting*

279 To estimate the number of nests as a function of the mapped nest area for each colony, we  
280 used a predictive modelling framework. We first summarised the number of manually  
281 counted nests and the mapped nest area within each 50 x 50 m quadrat. We then predicted the  
282 number of nests in each quadrat, with the whole colony count being the sum of the quadrat  
283 estimates. We used two simple approaches: 1) an assumption that the number of nests is  
284 directly proportional to the mapped nest area (linear area:count ratio) and 2) a generalised  
285 linear model (GLM; Poisson error distribution) of nest count as a function of nest area and  
286 local nest density; we expected that the local density of nests would have a relationship to the  
287 number of nests. Density was calculated as the percentage of the 50 x 50 m quadrat mapped  
288 as nests. Using a GLM with a negative binomial error distribution or a generalised additive  
289 model with smoothers for nest area and density provided no appreciable gains, so were not  
290 pursued further.

291

292 We used a resampling procedure to examine the number of manually counted 50 x 50 m  
293 quadrats needed to accurately estimate the number of nests for a whole colony. This involved  
294 repeated random sampling of  $n$  quadrats, estimating the number of nests using the area ratio  
295 and GLM approaches described above. We used 800 iterations without replacement (i.e.  
296 Monte Carlo resampling, not a bootstrap) for each of 1, 2, ...,  $n_{max}$  quadrats. This resulted in a  
297 sampling distribution of 800 whole-colony nest count estimates at each  $n$ .

298

299 To simulate the scenario of having limited resources for manual counting, we implemented  
300 another resampling approach to determine whether a given sample of the manually counted

301 quadrats can provide an accurate estimate (plus a confidence interval) of nest count for a  
302 whole colony. This involved a random draw of  $n$  quadrats (i.e. scenario of choosing a set of  
303 quadrats for training), and applying a repeated  $k$ -fold cross-validation using the area ratio and  
304 GLM estimation approaches. Each random draw of quadrats was stratified by mapped nest  
305 area density, to simulate choosing a range of nest density quadrats to count. We used  $k = 10$   
306 and 10 repeats for the cross-validation, and varied  $n$  from ~10-40% of the total number of  
307 manually counted quadrats. This resulted in a sampling distribution of 100 nest count  
308 estimates for each random draw of quadrats, and we took the mean as the resampling estimate  
309 and 2.5 and 97.5 percentiles as a 95% confidence interval. We decided on  $k$ -fold resampling  
310 as a good approach to reduce bias for the small sample sizes, but a range of resampling  
311 options are available (Lyons *et al.* 2018b). All statistical analysis was performed in R version  
312 3.5.1 ((Team 2018); see Data accessibility section).

313

### 314 **3 Results**

#### 315 *3.1 Manual training and validation nest counts*

316 The four study colonies varied widely in size, number of nests and bird density (Table 1). The  
317 flying height of ~100 m generated orthomosaic imagery with a pixel size between 3 – 4 cm. It  
318 took between 5 – 15 minutes to manually count the nests in a 50 x 50 m quadrat, with higher  
319 nest density on the upper end of that time. Ibis nests and the flooded colony environment are  
320 so variable that it was often not possible to accurately manually count nests, even in 3 – 4 cm  
321 pixel drone imagery. Occasionally, artefacts from drone imagery processing also obstructed  
322 counting. The accuracy of the manual counting was estimated using the on-ground counts,  
323 which ranged from  $\pm 6\%$  to  $\pm 12\%$  (Table 1). The largest colony had a manual count of 96,989  
324 nests, and with an estimated population of over 200,000 birds at the time (Lyons *et al.*  
325 2018a), regardless of the counting error, it is one of the biggest ever to be monitored via  
326 drone.

327

### 328 3.2 Semi-automated approach

329 The exact same Google Earth Engine code was able to be applied to each colony, showing  
330 that the nest area mapping routine was robust to the differing conditions and targets within  
331 and among each of the colonies. We found that around 10 of the 30 m training buffer areas  
332 were required for consistent classification of the large extent colonies (*Merrimajeel*, *Zoo*  
333 *Paddock*; ~5% total area), and around 5 for the smaller extent colonies (*Eulimbah*, *Block*  
334 *Bank*; ~10% total area). Our assessment of consistent was relatively ad hoc, using a visual  
335 assessment of whether nests and background were well separated. We opted to leave a  
336 quantitative assessment of accuracy for the subsequent nest count estimation. Figure 2 shows  
337 some examples of the metrics used as predictors for the random forest classifier, and Figure 3  
338 shows an example of the classified nest area for each colony.

339

340 The first resampling routine demonstrated that there was quite a large amount of variation in  
341 nest estimates given any random draw of quadrats, but that only a much smaller subset of the  
342 quadrats was required to capture most of the variation (Supplementary Fig. 1). There was no  
343 noticeable gain in using the GLM estimation method over the straight area ratio method.  
344 Inspecting the results of the nest count estimates for individual quadrats showed that there  
345 was a large amount of variation among estimates for individual quadrats, further motivating  
346 the use of a resampling-based estimate (Supplementary Fig. 2).

347

348 For the  $k$ -fold nest count estimation, we decided that an adequate number of quadrats ( $n$ ) to  
349 use would be signified by most of the estimates from each  $k$ -fold cross-validation falling  
350 within the error margin of the manual nest counting. For the two largest colonies,  
351 *Merrimajeel* and *Zoo Paddock*, we judged that to be 30 quadrats (~12% of all 50 x 50 m  
352 quadrats) to provide accurate estimates. For the two smaller colonies, *Eulimbah* and *Block*

353 *Bank*, we judged that to be 10 and 15 quadrats respectively (~20% and ~30% of total quadrats  
354 respectively). Figure 4 shows the  $k$ -fold nest count estimates (compared to manual count and  
355 error margin) for a set of 40 random draws for each of the colonies. The estimation was most  
356 accurate for the smaller two colonies. Again, there was no noticeable gain in using the GLM  
357 estimation method over the straight area ratio method; the gain from stratifying the random  
358 draw by mapped nest density was far more appreciable.

359

360 Parameterisation and thresholds for what is adequate will vary with the requirements for  
361 monitoring outcomes. The code provided allows users to fully customise the amount of  
362 training data for the random forest classifier and its internal parameterisation, the number of  
363 quadrats to sample for nest count estimation, the number of random draws to perform, the  $k$   
364 for  $k$ -fold and the number of  $k$ -fold repeats (see Data accessibility section).

365

#### 366 **4 Discussion**

367 The aim of this study was to develop a generalised approach that could map and count a key  
368 population metric – the number of nests – in four large and complex bird colonies using  
369 remotely sensed data captured via drones. An underlying driver was for the approach to be  
370 simple and robust enough to be applied in multiple environments, and modular such that  
371 users could readily change parameters or substitute their own or more appropriate methods as  
372 needed. We demonstrated a semi-automated approach founded on applying a machine  
373 learning classifier to high-resolution drone imagery to identify nests, and a modelling method  
374 to estimate a nest count. The methods were able to be applied exactly the same across all four  
375 colonies, and we found that only a relatively small amount of training data was required to  
376 estimate nest numbers with similar accuracy to manually counting from the drone imagery.

377

378 *Cost-benefit of the semi-automated approach*

379 The two key motivators for drone-based automated methods are reducing (on-ground) human  
380 observer bias and reducing human-input time (Chabot & Bird 2015; Baxter & Hamilton  
381 2018; Hodgson *et al.* 2018; Hollings *et al.* 2018). For very large and complex aggregations,  
382 like the bird colonies we surveyed, it is rarely possible to perform comprehensive on-ground  
383 counts. The primary motivator for automated methods is saving time. As we reported, our  
384 automated method provided significant time-savings. For example, it took ~40 hours to  
385 manually count all nests in the *Merrimajeel* colony, but ~5 hours to count enough nests to  
386 provide the same estimates using the *k*-fold cross-validation method (~8x faster). The time  
387 saving was less attractive for the smaller colonies; for example, the semi-automated approach  
388 was ~3.5x faster at *Block Bank*.

389

390 Explicitly quantifying cost-benefit is difficult, due to varying user ability and conditions  
391 across the whole exercise, including data acquisition in the field, drone image processing,  
392 modelling and programming, and even the level of detail and accuracy required for  
393 monitoring outcomes. While cost-benefit will improve over time, we concede that the  
394 realised benefits will vary between users. For example, if just a one-off monitoring exercise is  
395 required, then the most cost-effective option for users without prior experience, in terms of  
396 resources and delivery-time, is probably to just manually count features. Lowering the  
397 processing and skill overheads for applying automated methods is the critical factor for  
398 improving the cost-benefit ratio.

399

400 *Advantages and challenges for increased uptake of automated methods*

401 Transferability across environments and spatial scales has been identified as a key limitation  
402 preventing the uptake of automated methods within the broader scientific and management  
403 communities (Chabot & Francis 2016; Hollings *et al.* 2018). Using our semi-automated



404 approach, the exact same routine/code was applied to each colony, which will facilitate easier  
405 transfer for other users on their own data. Large variation in target and background features,  
406 potentially combined with processing artefacts, results in high spatial variation in target  
407 features across the imagery. Most current detection approaches that are more algorithmic in  
408 how they treat colour and shape of target features naturally rely on consistency in their colour  
409 and shape, as well as consistency of the target background. The random forest classifier  
410 enabled efficient handling of redundant predictor data (Breiman 2001), which provides  
411 capacity to account for a range of spatial and spectral variation in target features, as well as  
412 potential image blur and illumination artefacts (Fig. 3, top row).

413

414 Recent research beginning to tackle this issue of consistency across target and background  
415 features has also used a remote sensing mapping mentality (e.g. (Afán, Máñez & Díaz-  
416 Delgado 2018; Chabot, Dillon & Francis 2018)). The ability to apply a single consistent  
417 detection routine to multiple cases will be a key factor for broader uptake across scientific  
418 and management applications (Hollings *et al.* 2018). It is important to note though that  
419 approaches like Descamps *et al.* (2011) and Hodgson *et al.* (2018) require less training data  
420 than the approach we developed here. Thus they represent more significant time savings if  
421 they can be further developed to work across larger spatial extents.

422

423 Similarly to that demonstrated in (Chabot, Dillon & Francis 2018), we think a mapping  
424 driven mentality represents increased ability to deal with large volumes of image data. Many  
425 existing methods deal with image tiles in the order of 1-10 Mb. The bird colonies we  
426 surveyed are in the order of 500 Mb to 5 Gb, so existing methods may require significant  
427 modification to perform efficiently, if at all. Use of the Google Earth Engine platform enables  
428 handling of large data, and will allow future expansion into web-based tools where users only

429 supply imagery and training data, reducing local expertise and computing resource  
430 requirements.

431

432 Our approach was successful for identifying nest material as well as individual birds when  
433 they were captured in imagery away from their nests (see Fig. 3, 3<sup>rd</sup> row). This demonstrates  
434 that a mapping driven approach would also be suitable for identifying individuals if that was  
435 a main aim. Indeed (Chabot, Dillon & Francis 2018) successfully used an object-based  
436 mapping approach for identifying and counting individual Snow Geese. For small and simple  
437 tasks (e.g. counting just a few thousand birds or nests) the  $k$ -fold estimation process we used  
438 could be replaced with simple thresholding or classification of the predictor metrics. For  
439 example, thresholding and vectorizing the predictor layers in Figure 2 (e.g. bottom row)  
440 would produce very accurate counts, but the thresholds become too variable to apply  
441 consistently as spatial scale increases.

442

443 For the colonies that we surveyed, mapping the nest area required about a third of the training  
444 data needed to estimate the actual nest counts. This is important because for some monitoring  
445 applications, mapping the area or location of the phenomenon may be sufficient, which  
446 increases the cost-benefit saving. The main challenge for our approach was converting the  
447 mapped area to nest estimates. Although generally successful, we were unable to rectify over  
448 estimation for the *Zoo Paddock* colony. This colony was a very large, but only sparsely  
449 populated. Further exploration of modelling methods that account for density might be  
450 beneficial for situations such as this.

451

452 A potential limitation of our approach is that uncertainty in the manual counting stage can  
453 propagate through to the mapping and counting stages. One of the challenges when  
454 transferring automated methods to larger spatial scales or more complex environments is

455 variation in image quality (Hollings *et al.* 2018). Indeed, our surveys were in flooded  
456 wetlands that had limited access points and take-off/landing was challenging. The remoteness  
457 and ethics requirements also dictated limited time in the colony itself. Together, this resulted  
458 in imagery being acquired across a wide range incident sun angles and during sub-optimal  
459 wind conditions. Resulting artefacts, like sun glint and image blur, occasionally inhibited  
460 manual counting. Older nests (e.g. Fig.1, top and bottom rows) are more difficult to identify,  
461 which attributed to manual counting errors up to ~12%. The cross-validation method we  
462 implemented does a good job at accounting for this error (Fig. 4, Supplementary Fig. 1 & 2),  
463 but also leads to the need for larger amounts of training data.

464

#### 465 *Managing expectations for drone-based monitoring*

466 An unintended side effect of the intense focus on accurately counting individuals is backlash  
467 against the “drones vs. humans” attitude that a some of the literature presents. This idea is in  
468 fact a fallacy because drones don’t typically count anything at all – large amounts of human  
469 effort goes into collecting and processing drone imagery, deriving the training and test data,  
470 and developing the detection routines. Almost two decades ago Fraser *et al.* (1999) showed  
471 that aerial counting from a kite-mounted camera was more accurate than ground surveys, but  
472 it’s unlikely one would propose that kites count birds better than humans.

473

474 We suggest development of semi-automated approaches should focus on adaptability to  
475 deliver key monitoring indicators (Baxter & Hamilton 2018), and that detection methods  
476 themselves should aim for three main properties: 1) they use predictor data that is easily  
477 derived from common drone-based (or airborne) imagery, 2) they require minimal  
478 parametrisation among environments, and any parametrisation should be accessible to non-  
479 expert users, and 3) they are implementable on a platform that is widely available, does not  
480 require significant local computing resources, and can handle large volumes of image data.

481

482 Researchers and managers become excited about the proposition of fast and accurate  
483 counting, but invariably are disappointed when faced with the cold reality of using drones to  
484 monitor large and complex biological phenomena. Progress in the field is indeed rapid, but it  
485 is important that we continue to make progress without over-selling the capabilities of  
486 research- and consumer-grade drones. There is still much work to be done in terms of  
487 extracting complete end-to-end scientific and management applicable information from  
488 drone-based monitoring. Drones should be viewed as a tool to complement ecological and  
489 environmental monitoring practitioners, rather than a means to replace them.

490

## 491 **5 Data accessibility**

492 The nest mapping routines were implemented in the Google Earth Engine  
493 (<https://earthengine.google.com/>). All of the statistical analyses, including nest counting,  
494 were performed in the R programming environment (Team 2018). The Earth Engine and R  
495 code are available on Github (<https://github.com/mitchest/bird-colony-count-drones>) and  
496 archived on Zenodo (*eventual Zenodo DOI link*). Due to ecological sensitivity and being on  
497 private land, the raw drone data cannot be released publicly for most of the colonies, but the  
498 code provided includes the summarised data required to perform all the analyses in this  
499 paper. Part of the *Eulimbah* colony can be shown, and we have developed a web-app through  
500 the Earth Engine (<https://mitchest.users.earthengine.app/view/ibis-drone-count>) so that users  
501 can explore the drone data, the predictor variables and the nest map classification  
502 interactively.

503

## 504 **Acknowledgments**

505 Financial and logistical support grants (Australian Research Council LP150100972), the  
506 Commonwealth Environmental Water Office, the New South Wales Office of Environment

507 and Heritage, Bush Heritage Australia and local land owners. We operated under two animal  
508 ethics approvals from the University of New South Wales Animal Care and Ethics  
509 Committee (16/3B and 16/131B). **Author statement:** All authors contributed to study  
510 design, ML, CC, JM and KB carried out field work, ML, JW and NM led the data processing  
511 and statistical analysis, and all authors wrote the manuscript.

512

## 513 **References**

- 514 Afán, I., Máñez, M. & Díaz-Delgado, R.J.D. (2018) Drone Monitoring of Breeding  
515 Waterbird Populations: The Case of the Glossy Ibis. *2*, 42.
- 516 Anderson, K. & Gaston, K.J. (2013) Lightweight unmanned aerial vehicles will revolutionize  
517 spatial ecology. *Frontiers in Ecology and the Environment*, **11**, 138-146.
- 518 Baxter, P.W. & Hamilton, G. (2018) Learning to fly: integrating spatial ecology with  
519 unmanned aerial vehicle surveys. *Ecosphere*, **9**.
- 520 Bendig, J., Yu, K., Aasen, H., Bolten, A., Bennertz, S., Broscheit, J., Gnyp, M.L. & Bareth,  
521 G. (2015) Combining UAV-based plant height from crop surface models, visible, and  
522 near infrared vegetation indices for biomass monitoring in barley. *International*  
523 *Journal of Applied Earth Observation and Geoinformation*, **39**, 79-87.
- 524 Boyd, W.S. (2000) A comparison of photo counts versus visual estimates for determining the  
525 size of snow goose flocks. *Journal of Field Ornithology*, **71**, 686-690.
- 526 Breiman, L. (2001) Random forests. *Machine Learning*, **45**, 5-32.
- 527 Buckland, S.T., Burt, M.L., Rexstad, E.A., Mellor, M., Williams, A.E. & Woodward, R.  
528 (2012) Aerial surveys of seabirds: the advent of digital methods. *Journal of Applied*  
529 *Ecology*, **49**, 960-967.
- 530 Callaghan, C.T., Brandis, K.J., Lyons, M.B., Ryall, S. & Kingsford, R.T. (2018) A comment  
531 on the limitations of uavs in wildlife research—The example of colonial nesting  
532 waterbirds. *Journal of Avian Biology*.
- 533 Caughley, G. (1977) Sampling in Aerial Survey. *Journal of Wildlife Management*, **41**, 605-  
534 615.
- 535 Chabot, D. & Bird, D.M. (2012) Evaluation of an Off-the-shelf Unmanned Aircraft System  
536 for Surveying Flocks of Geese. *Waterbirds*, **35**, 170-174.
- 537 Chabot, D. & Bird, D.M. (2015) Wildlife research and management methods in the 21st  
538 century: Where do unmanned aircraft fit in? *Journal of Unmanned Vehicle Systems*, **3**,  
539 137-155.
- 540 Chabot, D., Craik, S.R. & Bird, D.M. (2015) Population Census of a Large Common Tern  
541 Colony with a Small Unmanned Aircraft. *Plos One*, **10**.
- 542 Chabot, D., Dillon, C. & Francis, C.M. (2018) An approach for using off-the-shelf object-  
543 based image analysis software to detect and count birds in large volumes of aerial  
544 imagery. *Avian Conservation and Ecology*, **13**.
- 545 Chabot, D. & Francis, C.M. (2016) Computer-automated bird detection and counts in high-  
546 resolution aerial images: a review. *Journal of Field Ornithology*, **87**, 343-359.
- 547 Descamps, S., Bechet, A., Descombes, X., Arnaud, A. & Zerubia, J. (2011) An automatic  
548 counter for aerial images of aggregations of large birds. *Bird Study*, **58**, 302-308.
- 549 Drever, M.C., Chabot, D., O'Hara, P.D., Thomas, J.D., Breault, A. & Millikin, R.L. (2015)  
550 Evaluation of an unmanned rotorcraft to monitor wintering waterbirds and coastal

- 551 habitats in British Columbia, Canada. *Journal of Unmanned Vehicle Systems*, **3**, 256-  
552 267.
- 553 Evans, L.J., Jones, T.H., Pang, K.Y., Saimin, S. & Goossens, B. (2016) Spatial Ecology of  
554 Estuarine Crocodile (*Crocodylus porosus*) Nesting in a Fragmented Landscape.  
555 *Sensors*, **16**.
- 556 Fraser, W.R., Carlson, J.C., Duley, P.A., Holm, E.J. & Patterson, D.L. (1999) Using kite-  
557 based aerial photography for conducting Adelie penguin censuses in Antarctica.  
558 *Waterbirds*, **22**, 435-440.
- 559 Gorelick, N., Hancher, M., Dixon, M., Ilyushchenko, S., Thau, D. & Moore, R. (2017)  
560 Google Earth Engine: Planetary-scale geospatial analysis for everyone. *Remote  
561 Sensing of Environment*, **202**, 18-27.
- 562 Groom, G., Petersen, I.K., Anderson, M.D. & Fox, A.D. (2011) Using object-based analysis  
563 of image data to count birds: mapping of Lesser Flamingos at Kamfers Dam, Northern  
564 Cape, South Africa. *International Journal of Remote Sensing*, **32**, 4611-4639.
- 565 Haralick, R.M. (1979) Statistical and Structural Approaches to Texture. *Proceedings of the  
566 Ieee*, **67**, 786-804.
- 567 Hodgson, J.C., Mott, R., Baylis, S.M., Pham, T.T., Wotherspoon, S., Kilpatrick, A.D.,  
568 Segaran, R.R., Reid, I., Terauds, A. & Koh, L.P. (2018) Drones count wildlife more  
569 accurately and precisely than humans. *Methods in Ecology and Evolution*, **9**, 1160-  
570 1167.
- 571 Hollings, T., Burgman, M., van Andel, M., Gilbert, M., Robinson, T. & Robinson, A. (2018)  
572 How do you find the green sheep? A critical review of the use of remotely sensed  
573 imagery to detect and count animals. *Methods in Ecology and Evolution*, **9**, 881-892.
- 574 Kingsford, R.T. & Porter, J.L. (2009) Monitoring waterbird populations with aerial surveys -  
575 what have we learnt? *Wildlife Research*, **36**, 29-40.
- 576 Liu, C.C., Chen, Y.H. & Wen, H.L. (2015) Supporting the annual international black-faced  
577 spoonbill census with a low-cost unmanned aerial vehicle. *Ecological Informatics*, **30**,  
578 170-178.
- 579 Lyons, M., Brandis, K., Callaghan, C., McCann, J., Mills, C., Ryall, S. & Kingsford, R.  
580 (2018a) Bird interactions with drones, from individuals to large colonies. *Australian  
581 Field Ornithology*, **35**, 51-56.
- 582 Lyons, M., Brandis, K., Wilshire, J., Murray, N., McCann, J., Kingsford, R. & Callaghan, C.  
583 (2019) A protocol for using drones to assist monitoring of large breeding bird  
584 colonies. *Australian Zoologist*, **in press**.
- 585 Lyons, M.B., Keith, D.A., Phinn, S.R., Mason, T.J. & Elith, J. (2018b) A comparison of  
586 resampling methods for remote sensing classification and accuracy assessment.  
587 *Remote Sensing of Environment*, **208**, 145-153.
- 588 Pimm, S.L., Alibhai, S., Bergl, R., Dehgan, A., Giri, C., Jewell, Z., Joppa, L., Kays, R. &  
589 Loarie, S. (2015) Emerging Technologies to Conserve Biodiversity. *Trends in  
590 Ecology & Evolution*, **30**, 685-696.
- 591 Polakowski, W.E., Cournoyer, D.A., Rogers, S.K., DeSimio, M.P., Ruck, D.W., Hoffmeister,  
592 J.W. & Raines, R.A. (1997) Computer-aided breast cancer detection and diagnosis of  
593 masses using difference of Gaussians and derivative-based feature saliency. *Ieee  
594 Transactions on Medical Imaging*, **16**, 811-819.
- 595 Sarda-Palomera, F., Bota, G., Padilla, N., Brotons, L. & Sarda, F. (2017) Unmanned aircraft  
596 systems to unravel spatial and temporal factors affecting dynamics of colony  
597 formation and nesting success in birds. *Journal of Avian Biology*, **48**, 1273-1280.
- 598 Seymour, A.C., Dale, J., Hammill, M., Halpin, P.N. & Johnston, D.W. (2017) Automated  
599 detection and enumeration of marine wildlife using unmanned aircraft systems (UAS)  
600 and thermal imagery. *Scientific Reports*, **7**.
- 601 Team, R.C. (2018) R: A language and environment for statistical computing.

602 Vermeulen, C., Lejeune, P., Lisein, J., Sawadogo, P. & Bouche, P. (2013) Unmanned Aerial  
603 Survey of Elephants. *Plos One*, **8**.

604

605

606

607 **Tables**

608 **Table 1.** Location and information on the surveyed bird colonies. All bird colonies were  
609 located within New South Wales, Australia. Nests were manually counted from the drone-  
610 based imagery. Ground-based nest count error is based on in situ counts cross-referenced  
611 with manual nest counts from drone imagery. \*From (Lyons *et al.* 2018a) – the estimated  
612 number of birds incorporates site-specific information.

<b>Location</b>	<b>Date</b>	<b>50 x 50 m quadrats in grid</b>	<b>Manual nest count</b>	<b>Manual nest count error</b>	<b>Estimated number of birds*</b>
Lachlan River (Merrimajeel)	Oct 2016	233	96,989	±6.1%	200-250,000
Macquarie Marshes (Zoo Paddock)	Nov 2016	244	20,411	±8.8%	40-50,000
Murrumbidgee River (Eulimbah)	Nov 2016	71	13,343	±8.4%	30-40,000
Lachlan River (Block Bank)	Sep 2017	33	7717	±12.1%	15-20,000

613

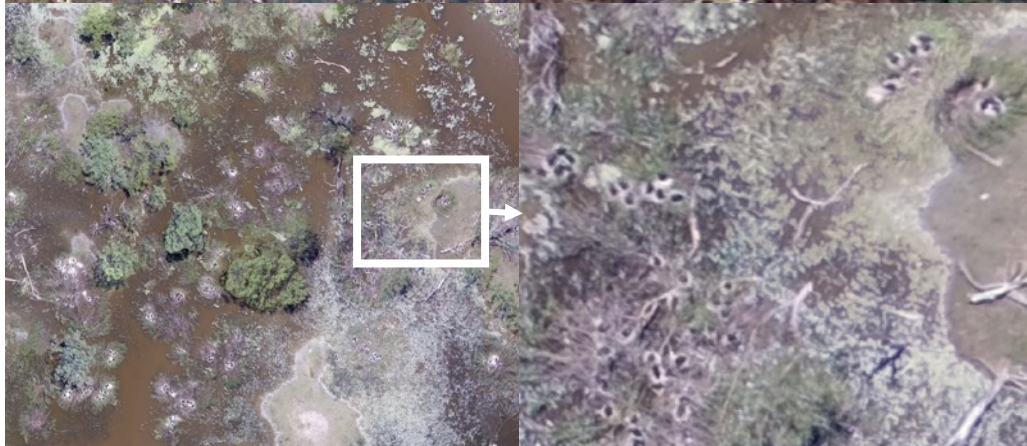
614

615

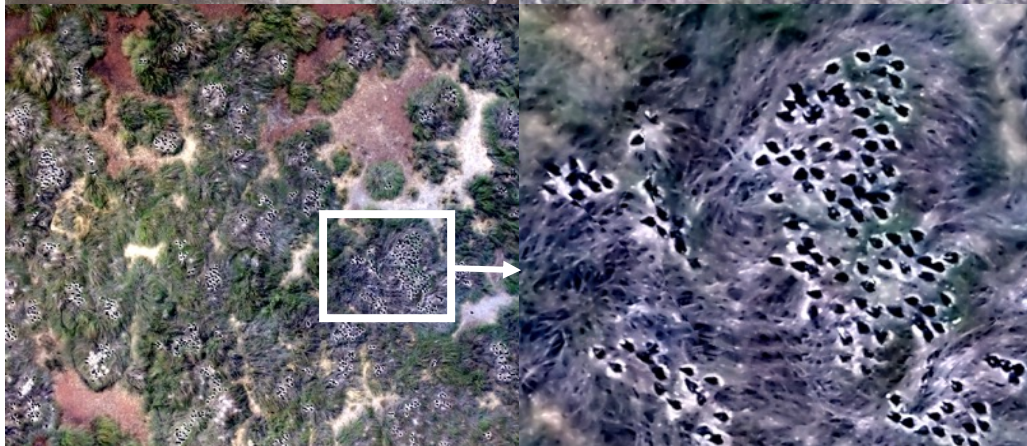
616 **Figures**



617



618



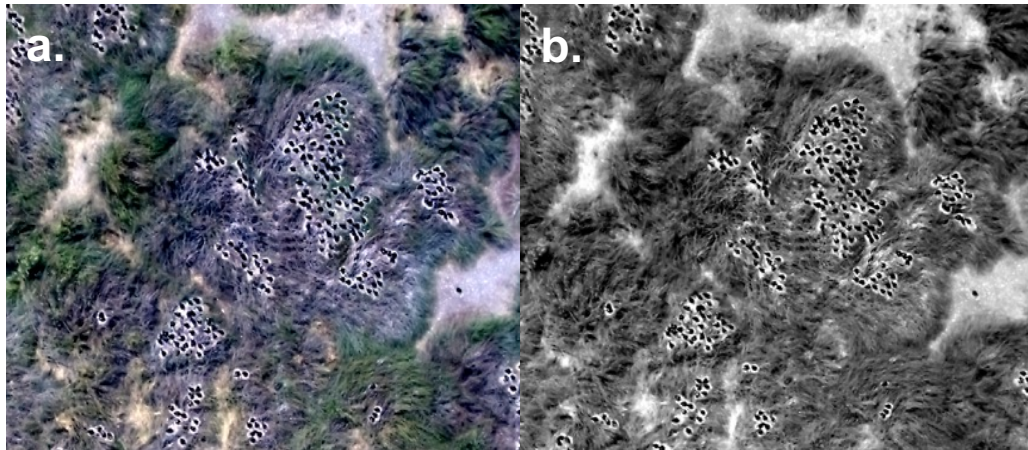
619



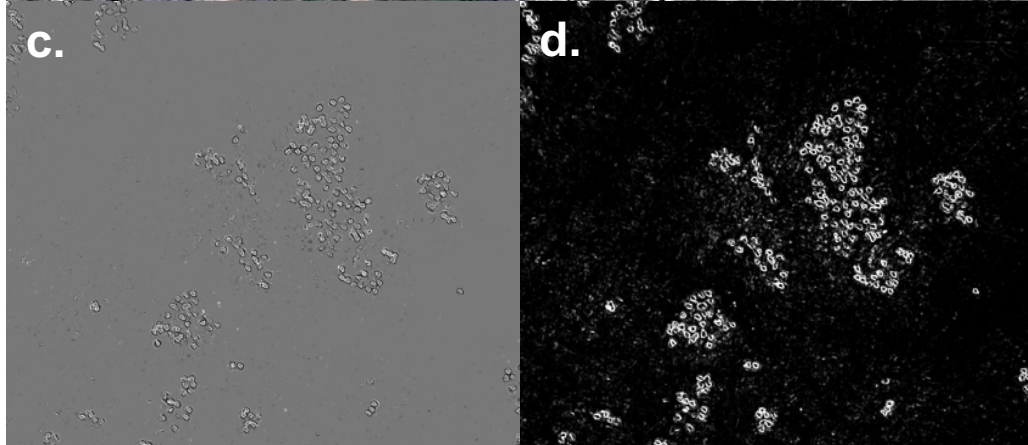
620  
621



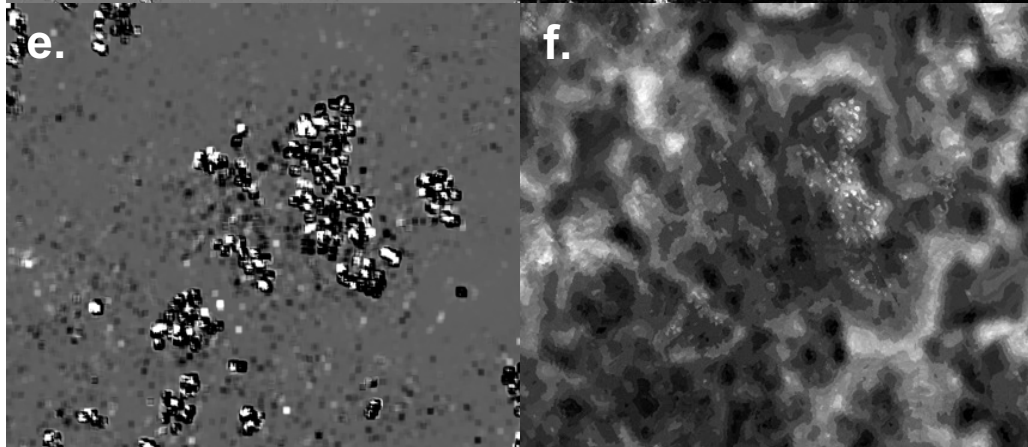
622 **Figure 1.** Example drone imagery showing the variation in nest types and environments  
623 across four breeding colonial waterbird colonies. Images from top row to bottom row are  
624 from the following colonies: *Merrimajeel*, *Zoo Paddock*, *Eulimbah* and *Block Bank*. Table 1  
625 gives location and size details for each of these colonies.  
626



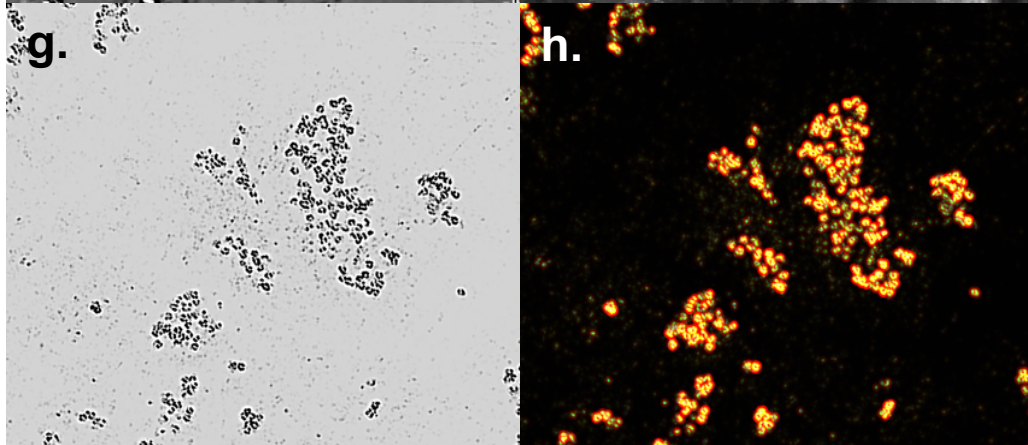
627



628



629



630  
631

632 **Figure 2.** An example of images metrics derived from drone imagery over a waterbird  
633 colony (*Eulimbah*) used as predictor variables in the random forest classification: **a** – raw  
634 drone imagery; **b** – ‘white’ brightness image; **c & d** – GLCM ‘shade’ and ‘contrast’ of the  
635 ‘white’ metric; **e** – GLCM ‘shade’ of the blue reflectance; **f** – RGB vegetation index; **g** –  
636 difference of gaussians applied to the GLCM ‘shade’ on the ‘white’ metric; **h** – an RGB  
637 composite of the ‘white’ metric and the standard deviation within a 2m and 7 m radius for the  
638 GLCM ‘shade’ of the ‘white’ metric. See ‘Data accessibility’ section for access to an online  
639 web-app to explore these layers interactively.  
640

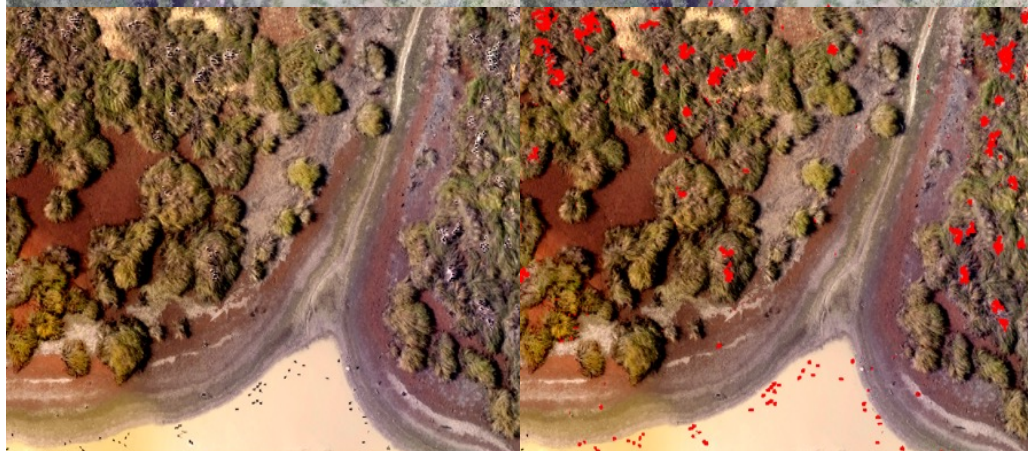
641



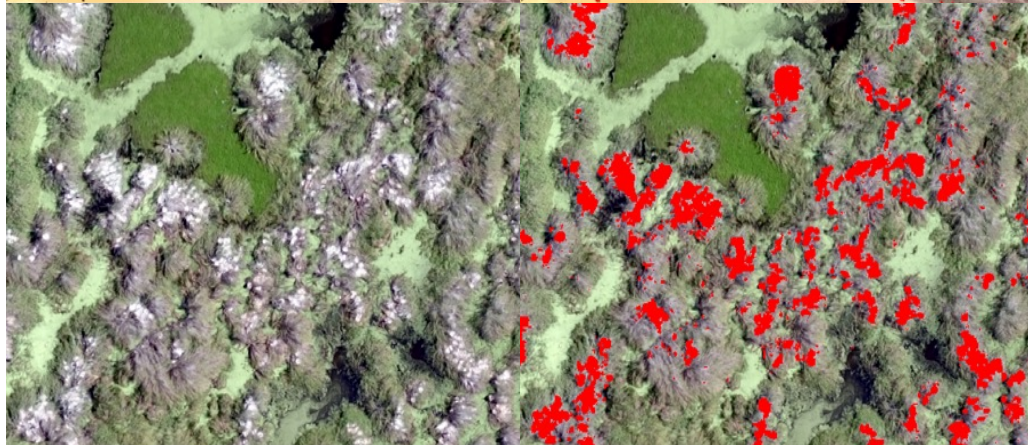
642



643



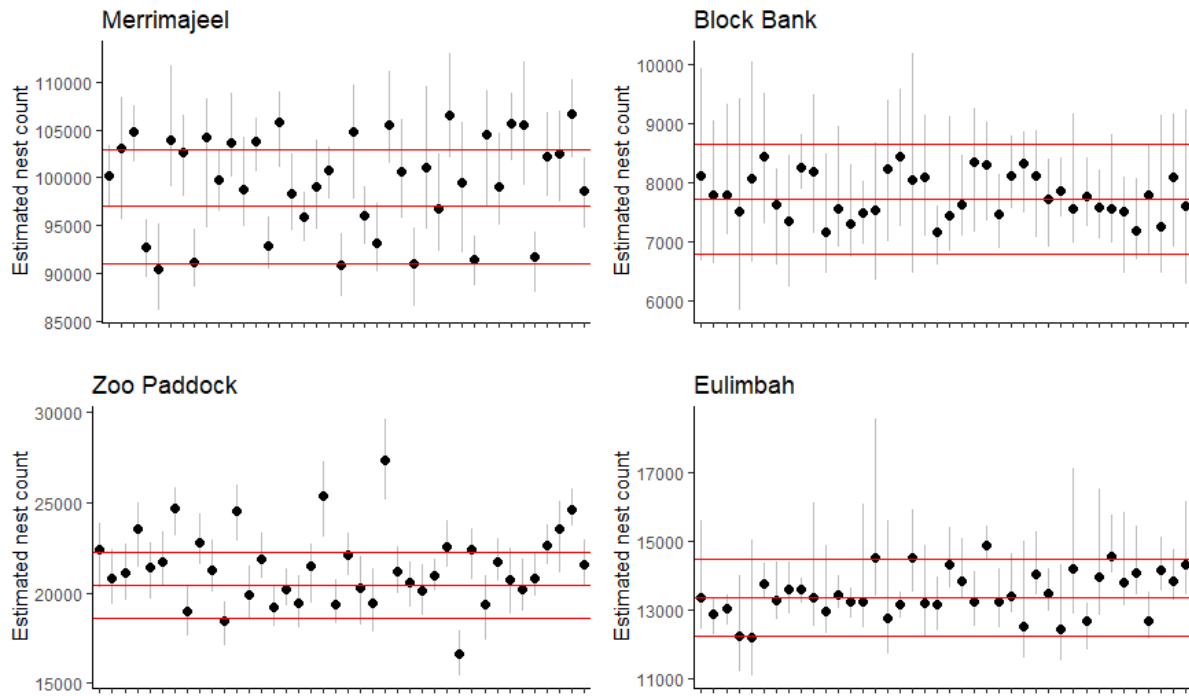
644  
645



646 **Figure 3.** Example nest area classifications for colonial waterbird colonies surveyed via  
647 drone and classified using a random forest classifier in the Google Earth Engine. Images from  
648 top row to bottom row are from the following colonies: *Merrimajeel*, *Zoo Paddock*, *Eulimbah*  
649 and *Block Bank*. Table 1 gives location and size details for each of these colonies. See ‘Data  
650 accessibility’ section for access to an online web-app to explore the *Eulimbah* layer  
651 interactively.

652

653

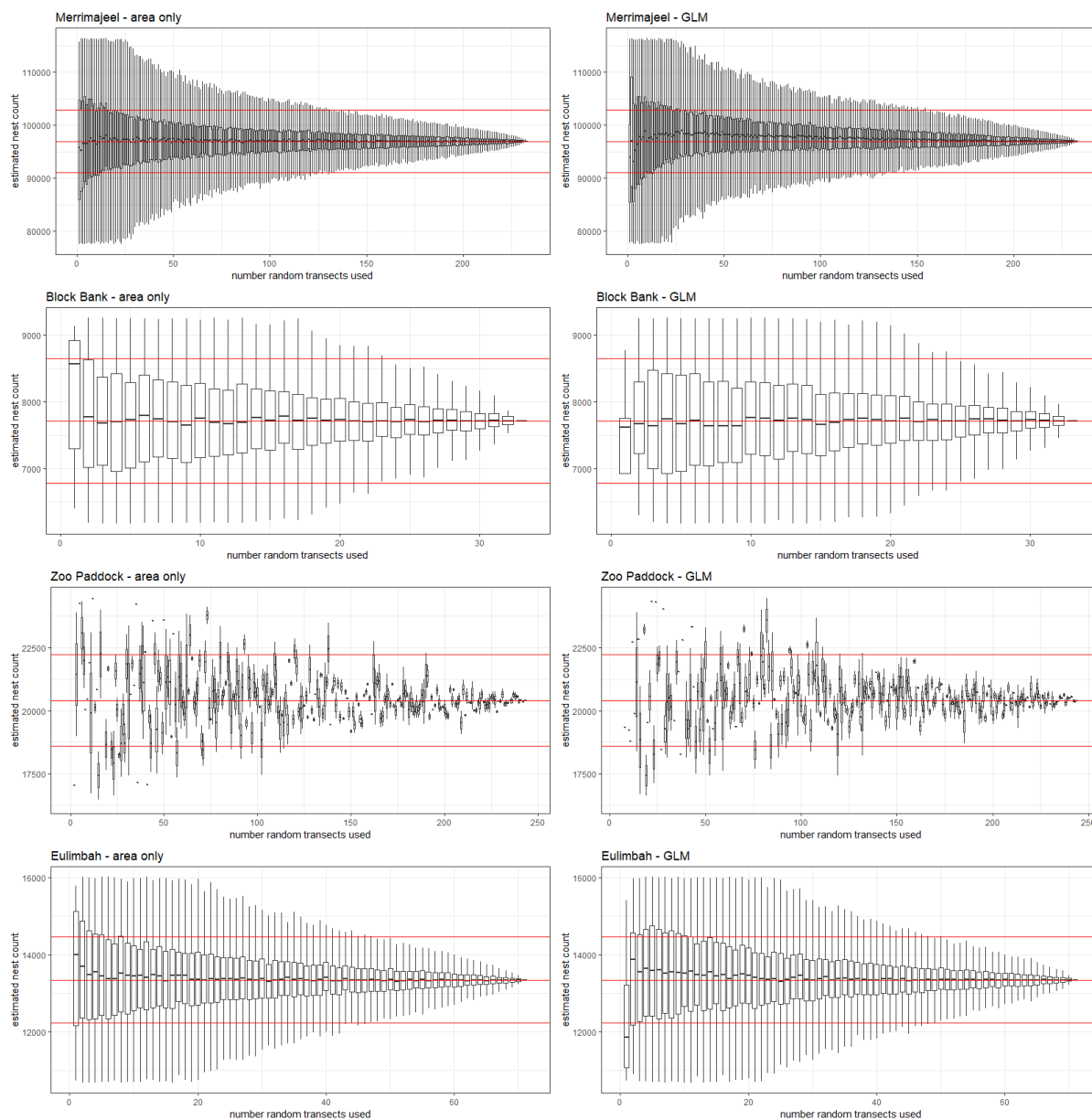


654

655 **Figure 4.** Resampling estimates of nest counts for breeding waterbird colonies surveyed via  
 656 drone, trained using a classification of nest area and manually counted nests. Each black dot  
 657 represents the mean of the sampling distribution (10x repeated  $k$ -fold  $k=10$  cross-validation)  
 658 for a different subset of the manually counted training nests (corresponding lines denote 95%  
 659 percentile), and the red horizontal lines denote the manual estimate for the whole colony, and  
 660 the 95% error margin calculated from on-ground counts.

661

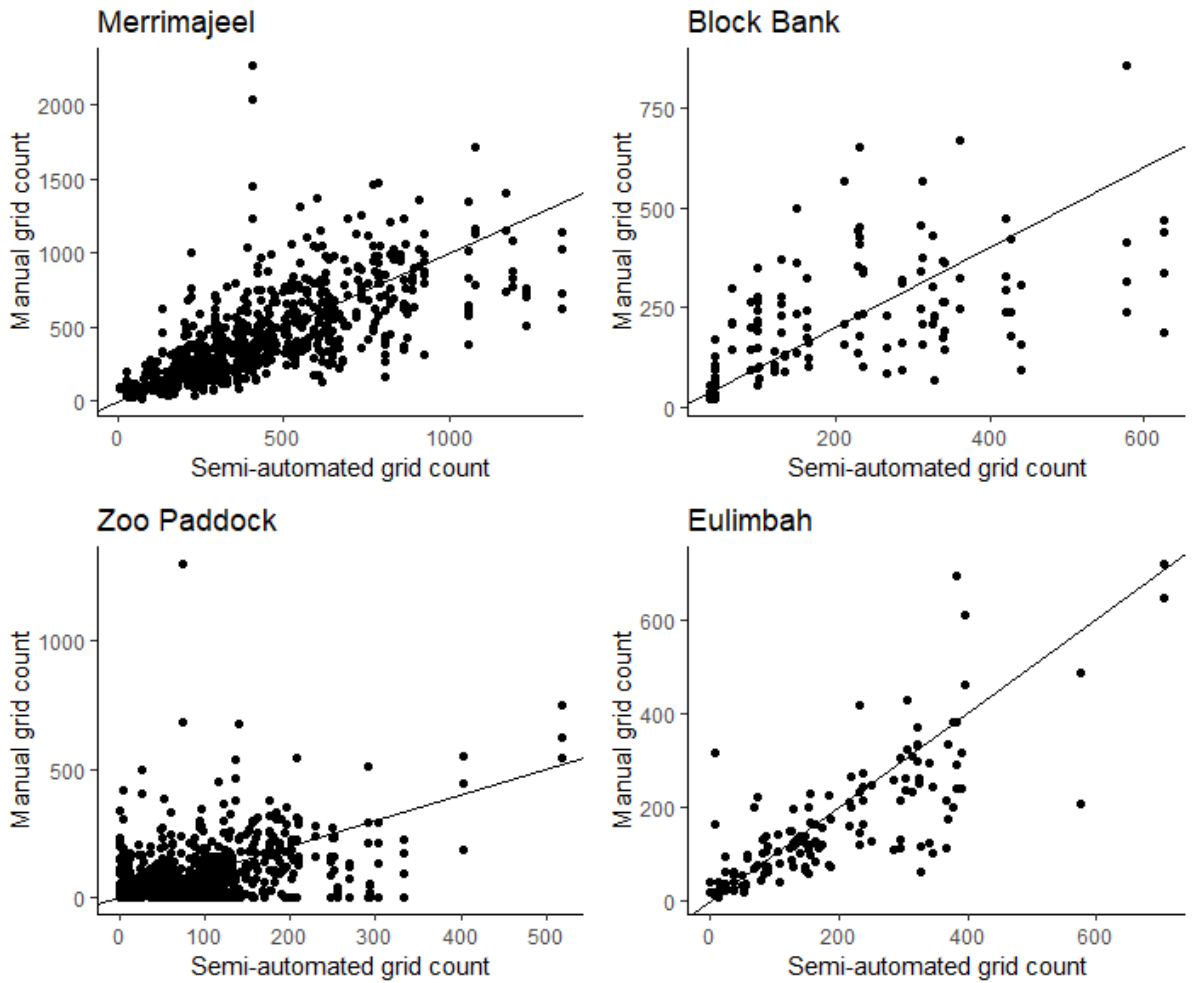
662 **Supplementary Material**



663

664 **Supplementary Figure 1.** Resampling estimates of nest counts for breeding waterbird  
665 colonies surveyed via drone, trained using a classification of nest area and manually counted  
666 nests (area ratio method on left and GLM method on right). Each box plot represents the  
667 sampling distribution (800x Monte Carlo cross-validation) for a different subset of the  
668 manually counted training nests, and the red horizontal lines denote the manual estimate for  
669 the whole colony, and the 95% error margin calculated from on-ground counts.

670



671

672 **Supplementary Figure 2.** For breeding waterbird colonies surveyed via drone, an example  
 673 of individual quadrat area estimates from machine learning classifier plotted against the  
 674 manual count form the corresponding quadrat.

675

676